

Histomorphometric Evaluation of a Nanothickness Bioceramic Deposition on Endosseous Implants: A Study in Dogs

Paulo G. Coelho, DDS, PhD;* Giuseppe Cardaropoli, DDS, PhD;† Marcelo Suzuki, DDS;‡
Jack E. Lemons, PhD§

ABSTRACT

Purpose: The objective of this study was to evaluate the bone response to a nanothickness bioceramic ion beam-assisted deposition (IBAD) on endosteal implants in a canine model.

Materials and Methods: Alumina-blasted/acid-etched (control) and IBAD-modified (test) implants were characterized by scanning electron microscopy, X-ray photoelectron spectroscopy + ion beam milling, thin-film mode X-ray diffraction, and atomic force microscope. The implants were surgically placed in four dogs' proximal tibiae and remained for 2 and 4 weeks in vivo. Oxytetracycline (10 mg/kg) was administered for bone labeling 48 hours prior to euthanization. Following euthanization, nondecalcified thin sections were prepared for UV and transmitted light microscopy. The amount of bone labeling was evaluated along the length and away from the implant surface by means of a computer software. The % bone-to-implant contact (BIC) was determined for each specimen. One-way analysis of variance at 95% level of significance along with Tukey's post hoc multiple comparisons were utilized for statistical evaluation. The characterization showed Ca- and P-based amorphous coatings with a 20- to 50-nm thickness.

Results: In vivo results showed a significant increase in general and site-specific (to 0.5 mm from the implant surface) bone activity for the 4-week test implants compared with the control implants. Bone activity levels decreased as a function of distance from the implant surface for all groups. No significant differences in BIC were observed between groups.

Conclusions: This study showed that both surfaces were biocompatible and osteoconductive and that a time-dependent increase in osteoactivity occurred around the test implants.

KEY WORDS: animal model, bioceramic, implant surface, nanothickness, osteoactivity

INTRODUCTION

Since the term osseointegration was defined,¹⁻³ biomaterial and surgical research on dental implant systems have increased significantly, and further development is moving rapidly. A driving force for increases in the

number of dental and orthopedic implant research protocols is, in part, a desire to obtain prosthetic restorations that are capable of function that is more similar to natural sites. There is also a wish for the shortest time for treatment completion.^{4,5}

Different methods have been used in an attempt to enhance bone healing after device implantation, including bulk device design,⁵ additions of biologic compounds,⁶ and biomaterial surface modifications.⁴⁻¹² Among all engineering surface modifications for dental and orthopedic implants, the addition of calcium- and phosphorous-based materials as coatings has received significant attention.^{5,7-14} Such interest is in part because of the bioceramics' elemental composition, which presents the same basic components of natural bone and can be applied along the implant surfaces by various industrial processing methods.^{10,11}

*Adjunct professor, Department of Biomaterials and Biomimetics, New York University, New York, NY, USA; †assistant professor, Department of Implant Dentistry and Periodontology, New York University, New York, NY, USA; ‡assistant professor, Department of Prosthodontics, Tufts University School of Dental Medicine, Boston, MA, USA; §professor, Department of Prosthodontics and Biomaterials, University of Alabama at Birmingham School, Birmingham, AL, USA

Reprint requests: Dr. Paulo G. Coelho, Department of Biomaterials and Biomimetics, New York University, 345 24th Street, Room 804a, New York, NY 10020, USA; e-mail: pgcoelho@nyu.edu

© 2008, Copyright the Authors
Journal Compilation © 2008, Wiley Periodicals, Inc.

DOI 10.1111/j.1708-8208.2008.00122.x

Most commercially available bioceramic coatings are processed as a 20- to 50- μm -thick plasma-sprayed hydroxyapatite (PSHA) coatings.^{5,7,9–11,15} While enhanced *in vivo* bone-to-bioceramic bonding and bone-to-implant contact (BIC) magnitudes have been observed at early implantation times for PSHA-coated implants,^{5,7,9–12,15} studies have shown that coatings may be partially dissolved/resorbed after long periods in function.^{5,7,9,12} PSHA-manufactured coatings normally rely on mechanical interlocking between a grit-blasted or etched metallic surfaces and the ceramic-like PSHA material for physical integrity during implant placement and function.¹⁰ This specific interface between the bulk metal, metal oxide, and bioceramic coating has been regarded by some as a weak link, where adhesive and failures during insertion or after osseointegration have been reported to occur.^{10,11,15} Also, uniform coating composition and crystallinity is difficult to reproduce in large-scale manufacturing, and alterations of calcium to phosphorous atomic ratios throughout the coating surface along with differences in relative thickness may change coating dissolution/degradation rates *in vivo*.^{5,7–9}

In an attempt to improve on these circumstances, thin-film bioceramic coatings have been developed for implant surfaces through processes like sol-gel deposition,¹⁰ pulsed laser deposition,¹⁶ sputtering coating techniques,^{17,18} ion beam-assisted deposition (IBAD),^{7–9,19} and electrophoretic deposition.¹⁰ These techniques often apply substantially thinner coatings compared with PSHA coatings.¹⁰

Desirable features of thin-film coatings include substrate surface roughness maintenance, controlled composition, and thickness plus enhanced adhesion to the metallic substrate.^{5,7–10,19} Controlled composition and thickness achievable through any of these processes also influence coating dissolution *in vivo*,⁷ thereby potentially affecting the device's osteoconductivity at early implantation times.⁸ Dissolution may also expose the metallic substrate after some time has elapsed after surgical placement. Therefore, the possibility of having close bone contact to the implant metallic substrate after coating total dissolution may be an attractive feature of thin films. This close contact would avoid potential interfaces between bone, bioceramic, surface oxides, and implant substrate. From a theoretical standpoint, the absence of such interfaces is favorable for an implant device's long-term anchorage.^{5,7,8}

Animal studies including sputtering-coated⁷ and micrometer thickness bioceramic IBADs on titanium implants have demonstrated higher biomechanical fixation, bioactivity, and BIC compared with noncoated implants at early implantation times.^{7,8} Also, investigations comparing PSHA-coated implants to sputtering-coated and IBAD-coated implants have shown comparable mechanical fixation after 12 weeks of implantation time in dogs' femora.²⁰

Although substantial data have been published concerning the bone-biomaterial interface, several factors that influence the phenomena of osseointegration remain under active investigation (ie, implant-biofluid interactions, the elemental chemistry and structure of surface films after implantation, and the overall mechanisms and kinetics of bone response to implants). Therefore, there is a continued need for further characterization of bone physiology and kinetics of healing during and after implantation to provide comparisons between existing and new implant biomaterials and biomechanical designs.

The objective of this study was to analyze the early bone response to a test thickness calcium- and phosphorous-based IBAD (test) on titanium alloy versus an alumina-blasted/acid-etched (control) surface on endosseous implants.

MATERIALS AND METHODS

Implant cylinders of 4 mm in diameter by 10 mm in length were utilized in the present study. The implant groups included the test ($n = 19$, IBAD coating applied to the control alumina-blasted/acid-etched titanium alloy substrate) and the control ($n = 19$, noncoated alumina-blasted/acid-etched titanium alloy substrate).

Three implants per group ($n = 3$) were used for the series of analytical tools employed for surface physico-chemical characterization.

Scanning electron microscopy (SEM) (SEM, Philips XL 30, Philips, Eindhoven, the Netherlands) was performed at various magnifications under an acceleration voltage of 15 keV. To determine if the coating deposition resulted in surface microtexture alterations, surface roughness parameters (average roughness [R_a] and root mean square [RMS]) were determined in $20 \times 20 \mu\text{m}$ scans in different regions of the implant by an atomic force microscope (AFM) in contact mode using a Nanoscope IIIa Multimode system (Digital Instruments, Santa Barbara, CA, USA). A scanner with a maximum

125 μm horizontal and 5 μm vertical range, and a 200 μm Si_3N_4 cantilever tip with a force constant of 0.12 N/m was used.

Surface-specific chemical assessment was performed by inserting the implants into a vacuum transfer chamber and degassing it to 10^{-7} torr. The samples were then transferred under vacuum to a Kratos Axis 165 multitechnique XPS spectrometer (Kratos Analytical Inc., Chestnut Ridge, NY, USA). Survey and high-resolution spectra were obtained using a 165-mm mean radius concentric hemispherical analyzer operated at constant pass energies of 160 eV for the survey and 80 eV for the high-resolution scans. Survey scans were performed at various locations throughout the implant body. A built-in charge neutralizer was used when necessary to compensate for sample charge buildup during XPS analysis. All spectra were referenced to the adventitious carbon C1s set at a peak position of 285.0 eV.

For coating thickness measurement, a combination of depth profiling by XPS and ion beam milling (IBM) was utilized. Three disks of 25-mm diameter and 3-mm thickness were subjected to the bioceramic IBAD, utilizing the same deposition parameters utilized for the implants (coatings aiming at ~ 300 nm were processed to facilitate the calculation of the coating IBM etching rate). The bioceramic deposition was mechanically removed from the center of each disk to expose the metallic substrate, and an AFM in contact mode was utilized for direct coating thickness determination (three measurements per disk). Then, a 4 keV Ar^+ ion sputter gun was employed to etch the disk surface at 2-minute intervals, and repeated cycles of etching and XPS high-resolution scans were carried out until the base alloy components were detected. The approximate etching rate calculated for the IBAD coating was ~ 8 nm/min (~ 5 nm/min for SiO_2 standard). The depth profiling procedure was then performed for the three test implants at three different positions on the surface.

Coating crystallographic assessment was performed by thin-film mode X-Ray diffraction (TFXRD). The implants were scanned from 30 to 38 degrees 2 theta at 0.05 degrees step size (2-second time step), 45 kV accelerating voltage, and 40 mA current). The rationale for using this 2 theta range was because of the presence of an alpha-Ti peak at approximately 35.5 2 theta degrees, the presence of the highest intensity hydroxyapatite peaks (at 31 and 33 2 theta degrees), and other Ca- and

P-based phases commonly found in bioceramic-coated implants.^{11,21} The peaks location/intensity versus 2 theta degree output was compared with theoretical crystallographic calculations for alpha (hexagonal close packed) and beta (body centered cubic)-titanium, and other Ca- and P-based phases.

In Vivo Model and Surgical Aspects

The laboratory in vivo model was four midsize class A adult (closed bone growth plates) mongrel dogs in good health. The dogs were obtained and followed for a 2-week housing period before surgery and 4 weeks postoperatively. The project was conducted after IRB approval in an AALAC approved facility (#990804919) at the University of Alabama at Birmingham.

The surgical region was the proximal tibia, with four implants placed in each limb. The first implant was inserted 2 cm below the joint line at the central medial-lateral position of the proximal tibiae. The remaining devices were placed along a distal direction at distances of 1 cm from each other along the central region of the bone. Each dog provided a 2- and 4-week comparison for experimental and control surfaces for the four implant location through sequenced surgical procedures. The overall distribution of implants per animal compared an equal number (8 \times) of the test and control implants for each in vivo evaluation time. Oxytetracycline was administered one time (10 mg/kg IV) at 48 hours prior to euthanization to provide bone labeling for histomorphometric analysis.

Specimen Preparation

At sacrifice, the proximal tibia was exposed by sharp dissection, and the upper one-half of the limb was removed and contact radiographed to confirm implant location and orientation. The upper third of the tibiae was reduced to blocks with the implant in its center. The blocks were kept in 10% buffered formalin for a period of 3 weeks, dehydrated in a graded alcohol series, and were embedded in a methylmethacrylate-based resin (Technovit 7200®, Kulzer GmbH, Germany).²² The blocks were sectioned, grounded, and polished to ~ 30 - μm -thick sections in an automated system (EXAKT Apparatebau, Norderstedt, Germany).

Histomorphometric Analyses

For tetracycline label area fraction quantification, the nondecalfied sections were placed under an optical

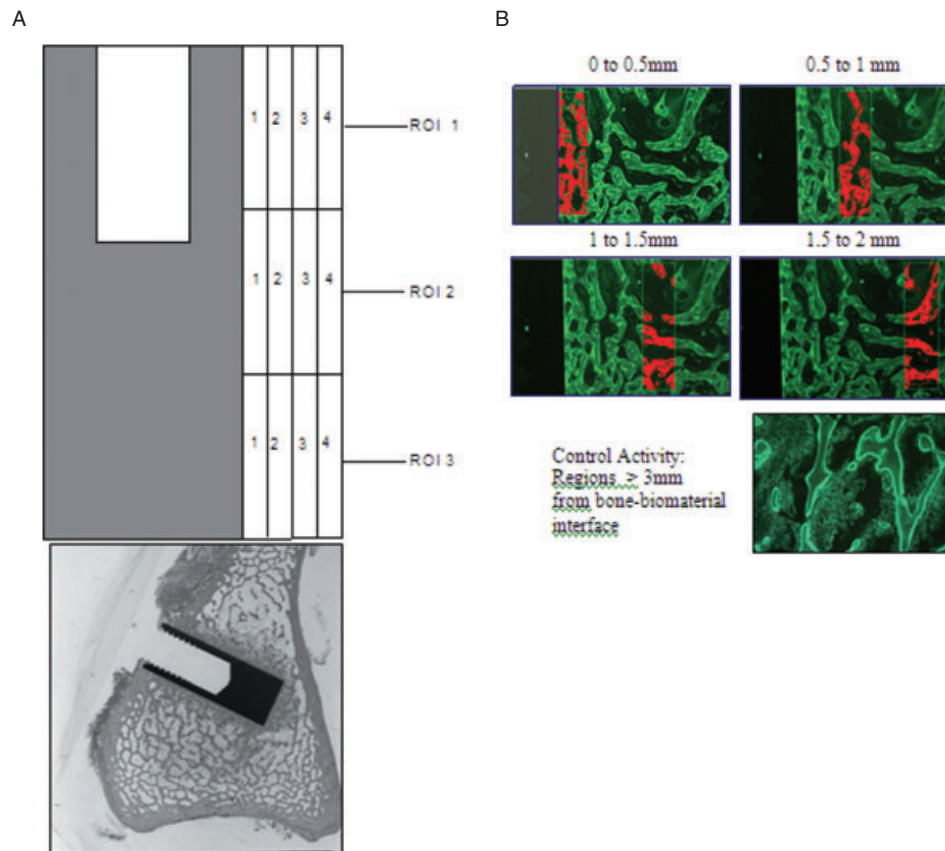


Figure 1 Schematic representation of regions of interest (ROIs) division around one implant side and data acquisition. *A*, schematic representation of the three ROIs on one implant side (both sides were evaluated on this experiment for each specimen) for implant full-length evaluation. Each ROI subdivision (1–4) had a base length of 0.5 mm, enabling labeling evaluation to 2 mm away from the bone–biomaterial interface. *B*, Image thresholding in 0.5-mm steps from the bone–biomaterial surface plus region of control activity data acquisition for one ROI.

microscope (Olympus, Melville, NY, USA) equipped with a UV light source and observed under a transmitted light mode including barrier filters. The magnification was $\times 40$, and a digital camera was used to capture sequential (by area) images of sample regions. The regions of interest (ROIs) were the two sides of the implant, and three images were required to obtain measurements from the entire implant length (Figure 1A). Each of the three images captured along the vertical direction was subdivided in four rectangles, with its smaller side representing 0.5 mm and its larger size representing approximately 3.3 mm of specimen length (see Figure 1A). This procedure enabled the evaluation of 2 mm of bone from the implant surface for each ROI.

Image thresholding was performed individually for each subdivision using a computer software (Bioquant NOVA, Bioquant Image Analysis Corporation, Nashville, TN, USA) (see Figure 1B). The labeled sites for both sides of the implant were evaluated according to their distance from the bone–biomaterial interface by

area fraction of the labeled bone. In order to evaluate the nonimplant site labeled bone activity area fraction, label measurements were obtained at control areas away from the implant site (more than 3 mm away from the surface) (see Figure 1B).

Measurements of BIC were obtained through microscopic measurements ($\times 80$ magnification) utilizing a computer software.

Statistical analyses were performed by one-way analysis of variance at the 95% level of significance for the various parameters evaluated. Tukey's post hoc multiple comparisons were performed for statistical evaluation.

RESULTS

Coating Characterization

The scanning electron micrographs at various magnifications did not depict physical evidence of a thin coating on the surface of the test, which presented surface topography similar to the control implants (Figure 2).

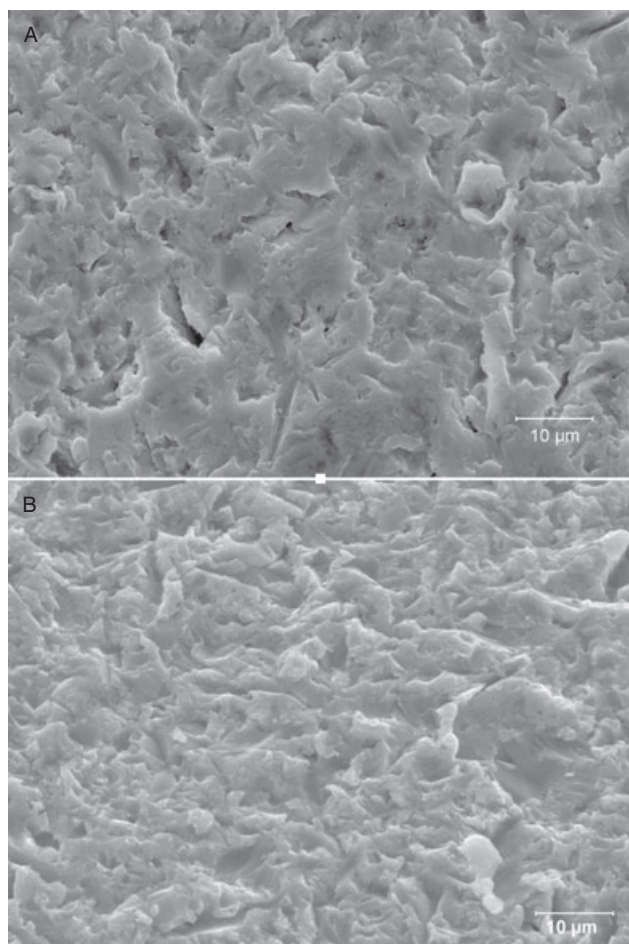


Figure 2 Scanning electron micrographs of the (A) control (alumina-blasted/acid-etched [AB/AE]) and (B) test (AB/AE + 20- to 50-nm thickness bioceramic deposition). Note that a coating could not be visualized because of its nanometric thickness dimension.

The scanning electron micrographs of all groups presented a topography commonly observed in blasted/etched surfaces.

The XPS survey analyses revealed the presence of O, C, Ca, and P for the test implants, and O, C, Ti, and Al for the control implants (Figure 3A). The coating thickness assessment utilizing the experimentally determined IBAD coating etching rate showed that coating thicknesses ranged from ~20 to 50 nm at different regions (because of the previous alumina-blasting/acid-etching texture of the surface and subsequent deposition, coating thickness was not uniform throughout the implant as thus the range as the evaluated parameter).

The TFXRD spectra showed no evidence of HA or any other Ca- and P-based phases (see Figure 3B). The only peak detected for both control and test implant surfaces was the alpha-Ti peak at 35.5 degrees 2 theta represented in Figure 3B.

The microtexture roughness parameters obtained from three $20 \times 20 \mu\text{m}$ scans for the different implant surfaces were not affected because of the coating deposition. The control implants presented (mean \pm 95% confidence interval) $R_a = 0.66 \pm 0.10 \mu\text{m}$ and $\text{RMS} = 0.45 \pm 0.07 \mu\text{m}$; the test implants presented (mean \pm 95% confidence interval) $R_a = 0.54 \pm 0.10 \mu\text{m}$ and $\text{RMS} = 0.52 \pm 0.10 \mu\text{m}$. The three-dimensional roughness profiles are presented in Figure 3, C and D. While a decrease in mean R_a and an increase in RMS values were observed due to the coating deposition, no significant differences between the control and test surface roughness parameters were observed.

Animal Follow-Up and Bone Distributions

Surgical procedures and follow-up demonstrated no complications regarding procedural conditions, post-operative infection, or other clinical concerns.

For most of the specimens, the first ROI (see Figure 1A) presented mostly cortical and a lesser amount of trabecular bone along the upper (entry site) analysis position. In few cases, the cortical bone was the only bone type present. The second ROI (toward the middle of bone) showed only trabecular bone along the implant for all specimens. The third ROI showed only trabecular bone in some cases, and in other a combination of cortical (opposite cortex) and trabecular bone. Direct bone contact along the implant surface was observed along most of the implant perimeter for all groups. Because of the coating thickness dimension (20–50 nm), no evidence of thin-film bioceramic coating was observed.

Tetracycline Labeling Distributions

All implants showed tetracycline labeling and revealed bone activity present within the local cortical, trabecular, and regional bone sites away from and along the bone–implant interface.

The overall bone-labeled area fraction was assessed independently (by location) and by adding all ROIs evaluated for each group. The summaries of means with 95% confidence intervals are shown in Table 1. Note that the overall magnitude of the labeled area fraction (osteactivity) for the 4-week test group was significantly higher compared with the remaining groups, where confidence intervals overlapped among each other and the normalizing group (general osteactivity levels) (see Table 1).

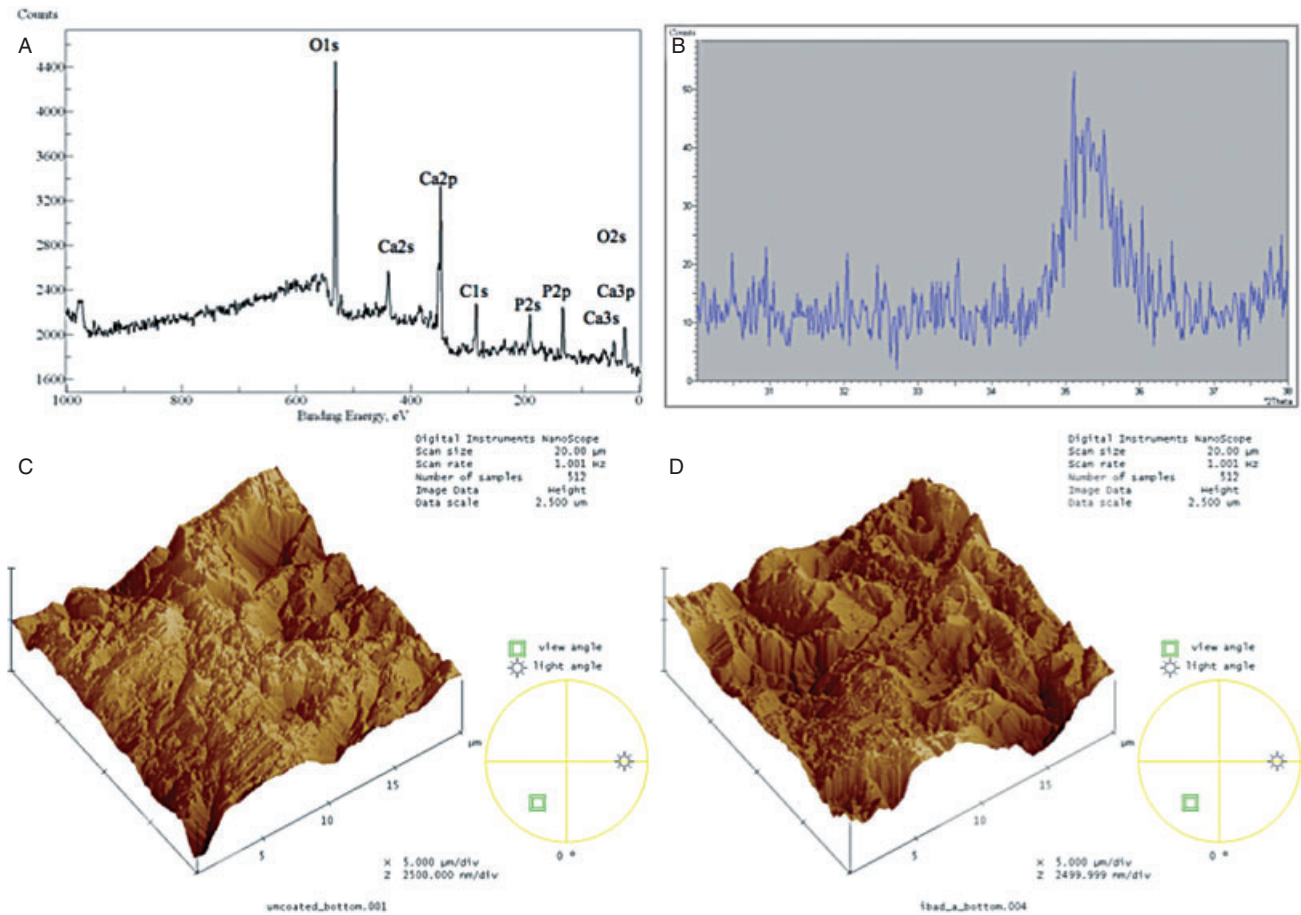


Figure 3 A, X-ray photoelectron spectroscopy spectrum showing the presence of Ca, P, O, and C on the surface of the test implant surface. B, Thin-film mode X-ray diffraction spectrum showing only the alpha-Ti peak and no peaks associated to Ca and P phases. C and D, Atomic force microscope depicting the surface texture of the (C) control and (D) test surfaces. Surface microtexture was not affected by the coating procedure.

Labeling results for the first, second, and third ROIs are also summarized separately for each group in Table 2. The highest osteoactivity values observed for the three ROIs were for the 4-week test groups. A common feature between the first and third ROIs was that the 4-week test group presented significantly higher values of the labeled area fraction compared with other

groups within each ROI. The other groups showed labeled area fraction values comparable to general (control) osteoactivity levels.

The evaluation of the second ROI individually showed that the 4-week control and test groups presented the highest levels of bone labeling, followed by an intermediate value for the 2-week test group. Note that the

TABLE 1 Table of Means with 95% Confidence Interval (CI) for Total Percent Labeling for Each Group

Group	Mean % Labeled	Lower Limit	Upper Limit
Control 2 weeks	13.10*	12.02	14.18
Control 4 weeks	12.35*	11.26	13.44
Test 2 weeks	12.66*	11.5	13.82
Test 4 weeks	17.16*	16	18.32
Normalizing	10.68*	9.3	12.06

*CI overlap groups.

TABLE 2 Ninety-Five Percent Confidence Intervals of the Total Amount Labeled (Percent) for the Different Groups for the First, Second, and Third Regions of Interest (ROIs) Plus Normalizing Group

Group	ROI	Mean % Labeled	Lower Limit	Upper Limit
Control 2 weeks	1	10.34 [†]	8.77	11.92
Control 4 weeks	1	12.09 [†]	10.52	13.65
Test 2 weeks	1	11.33 [†]	9.75	12.91
Test 4 weeks	1	18.76 [*]	17.19	20.34
Control 2 weeks	2	11.81 [†]	9.75	13.89
Control 4 weeks	2	15.92 [*]	13.85	18
Test 2 weeks	2	14.62 [*]	12.4	16.82
Test 4 weeks	2	19.34 [*]	17.11	21.57
Control 2 weeks	3	12.04 [†]	10.8	13.29
Control 4 weeks	3	10.56 [†]	9.32	11.81
Test 2 weeks	3	11.74 [†]	10.41	13.08
Test 4 weeks	3	16 [*]	14.67	17.33
Normalizing	N	10.68 [†]	9.3	12.06

*Confidence interval overlap groups within each ROI.

[†]Confidence interval overlaps with normalizing data.

N = region > 3 mm away from the implant surface.

confidence interval obtained for the 2-week test group overlapped with the 4-week control group and was significantly higher than the values obtained for the 2-week control group and general (control) levels of activity.

Further division of each ROI into four rectangles (see Figure 1A) provided an evaluation of bone labeling away from the implant surface in steps of 0.5 mm (see Figure 1B). The 0.5-mm steps for the three ROIs were evaluated together as a function of distance from the implant surface (Table 3). For all groups, the highest bone labeling values were found to be within the first 0.5 mm from the implant surface (the rectangle adjacent to the implant surface), and these values decreased as a function of distance from the implant. The labeling magnitudes dropped to general (control) activity levels before reaching the region between 1.5 and 2 mm. This drop to control labeling levels occurred after 0.5 mm away from the implant surface for the 2-week test and the 4-week control groups, and after 1 mm from the surface for the 2-week control and 4-week test groups (see Table 3).

The test implant groups showed higher values in the region adjacent to the implant surface compared with the titanium alloy groups at both times in vivo. However, only the 4-week test group presented significantly higher ($p < .03$) bone labeling levels compared with all other groups at the region adjacent to the implant surface (to 0.5 mm).

BIC

Summary statistics for BIC are presented in Table 4. This analysis showed no significant differences ($p > .43$) between the test and control groups at both follow-up times.

DISCUSSION

Implant dentistry clinical success is related to the implant biomaterial's ability to allow hard and soft tissue healing around the implanted device.¹ While dental implantology has success ratios reported above 90%, challenging clinical scenarios because of low bone density, atrophic alveolar ridges, or immediate loading protocol are often associated with lower success ratios.²³⁻²⁵ Thus, improvements in the system biomechanics through implant design because of increased biocompatibility, osteoconductivity, or osteoinductivity leading to faster/higher bone healing or turnover are highly desirable.²³⁻²⁵

Surface modifications through a variety of processes have resulted in increased amounts of BIC and biomechanical fixation at earlier implantation times compared with as-machined implants.^{13,14} These favorable results have been obtained through the alteration of surface roughness and chemistry. From a topography perspective, implant surface subjected to post-turning surface treatments yielding microtextured surfaces with R_a

TABLE 3 Ninety-Five Percent Confidence Intervals for Bone Activity as a Function of Distance from the Implant Surface

Group	Distance from the Surface (mm)	Mean % Labeled	Lower Limit	Upper Limit
Control 2 weeks	0.5	16.67*	14.6	18.73
	1	15.75*	13.68	17.81
	1.5	10.27†	8.2	12.34
	2	9.93†	7.8	12
Test 2 weeks	0.5	19.56*	17.66	21.46
	1	12.71†	10.81	14.62
	1.5	9.51†	7.61	11.41
	2	9.51†	7.61	11.41
Control 4 weeks	0.5	16.75*	14.78	18.73
	1	10.87†	8.89	12.85
	1.5	10.42†	8.44	12.4
	2	11.34†	9.36	13.32
Test 4 weeks	0.5	25.3*	23.07	27.53
	1	16.31*	14.09	18.54
	1.5	13.4†	11.17	15.63
	2	12.56†	10.78	14.33
Normalizing	>3	10.68†	9.3	12.06

*Confidence interval overlap groups within distances for each group in vivo.

†Confidence interval overlaps with normalizing data.

between 0.5 and 1.5 μm has been shown to increase the early host-to-implant response compared with as-turned implants.^{13,14,26} However, unlike the potential synergy between mechanical interlocking and chemical bonding involving thick PSHA-coated implants and bone, early fixation of uncoated devices relies primarily on mechanical interlocking between bone and substrate.^{13,14}

Calcium- and phosphorous-based thin-film processing in the range of ~1- to 5- μm thickness onto implant surfaces has become an alternative for dental

implant coatings, as its more controlled coating composition and adhesion to the metallic substrate may avoid problems associated with PSHA-coated devices after implantation.¹⁰ Nevertheless, while favorable biomechanical and histomorphometric results have been demonstrated through thin coatings of ~1- to 5- μm thicknesses,^{7,8,27,28} processing techniques may require highly specialized equipment and long processing times for their large-scale production, substantially increasing the cost per implant. Thus, if favorable results were achievable with bioceramic coatings in the

TABLE 4 Summary Statistics for the Percent Bone-to-Implant Contact Evaluation Parameter

Group	Mean Percent Bone Contact to Implant Surface	Lower Limit	Upper Limit
Control 2 weeks	85.57*	77.43	92.71
Control 4 weeks	87.13*	80	94.27
Test 2 weeks	73.38*	65.75	81.01
Test 4 weeks	87.19*	79.56	94.82

*Statistically homogeneous groups.

nanothickness range, large-scale production without substantial increase in treatment cost would be more easily achievable.

According to surface topography and chemistry parameters known to enhance osseointegration,^{3,4,10,25,27-29} nanothickness Ca- and P-based bioceramic coatings may be attractive for endosseous dental implants, as it may not significantly alter the substrate surface roughness (see Figures 2 and 3) while adding the biocompatible and highly osteoconductive properties of Ca- and P-based surface chemistry.^{10,25,29}

The combination of characterization techniques utilized in the present study showed that a thin bioceramic layer of thickness ranging from 20 to 50 nm covered a previously alumina-blasted/acid etched surface. While coverage throughout the surface by the bioceramic coating was detected by survey surface chemistry analysis, the coating thickness range at various implant regions likely resulted from the textured substrate morphology prior to deposition. Also, the 20 × 20 μm AFM scans showed that slight alterations in surface roughness parameters were observed after coating deposition (see Figure 3, C and D). Even though the effect of surface roughness in the nanometer scale has been speculated to result in bone bonding to the substrate,^{25,30} in vivo studies concerning controlled surface roughness in the micrometer and nanometer ranges are necessary to confirm bonding between bone- and substrate-specific magnitudes of surface roughness.

As previously reported^{7,10,31} for IBAD of bioceramic coatings without subsequent heat treatment, an amorphous microstructure was detected for the 20- to 50-nm-thick coatings (see Figure 3B).

The overall biologic assessment of the implant surfaces utilized in our experiment showed that the majority of specimens from all groups demonstrated intimate cortical and trabecular bone contact to the implant irrespective of implant surface supporting both surfaces' biocompatible and osteoconductive properties.¹⁻⁴ However, while acceptable biocompatible properties have been reported for Ti-6Al-4V in different studies,^{5,32} the utilization of commercially pure titanium implants would be desirable to better understand the behavior of bone around the IBAD-coated implants and to further investigate any potential differences in osseointegration as a function of alloy composition.

In this study, only one label was administered to the animals at 48 hours prior to euthanization for relative determination of osteoactivity (osteoblastic activity) at 2 and 4 weeks in vivo. The specimen division into ROI provided the evaluation of activity levels in regions of cortical and trabecular bone along the tibiae. The variation in anatomy between the ROIs was because of the different cortical-to-trabecular ratios along the implants sequentially placed away from the joint. The sequenced surgical procedures provided an equal number of specimens per group, animal, and surgical site (cortical-to-trabecular ratio), and time in vivo. The rationale for sequenced surgical procedures was to decreased histomorphometric comparison bias because of surgical site anatomy.

When the three ROIs along both implant sides were evaluated together for osteoactivity (see Table 1), bone around the 4-week test implants showed significantly higher levels compared with other groups, which overall levels overlapped with general osteoactivity (control- > 3 mm away from the surface). This time-dependent increase in osteoactivity was further supported by analyzing each ROI individually, where the 4-week test implants presented significantly higher osteoactivity levels at the first and third ROIs (regions where cortical bone was present). The same trend was also observed for the second ROI, where cellular content and morphology were different (trabecular bone). The bone labeling results supported a time-dependent increase in osteoactivity (osteoblastic response) for the test implant group and provided evidence of cortical and trabecular bone kinetics change at early implantation times because of the nanothickness¹⁹ deposition presence. These results suggest that bone modeling process^{5,33,34} is increased around the test implants and may enable earlier implant loading.

A decrease in osteoconductivity as a function of distance from the implant surface to general (control) levels was found for all groups evaluated (see Table 3). Labeling levels were highest for all groups at the region adjacent to the implant surface (to 0.5 mm). These results showed that a significant increase in activity (bone modeling) was confined to the first millimeter from the implant surface as previously reported for different animal models including humans.¹³⁻¹⁵ The significantly higher value of bone labeling at the region adjacent to the 4-week test implants (see Table 3) showed, once again, a time-dependent increase in osteoactivity.

It is accepted that bone modeling and subsequent remodeling at regions in proximity to the implant surface are responsible for the short- and long-term success of dental implants.^{33–35} Therefore, increases in osteoactivity levels at regions in proximity to the test implant surface may influence bone modeling/remodeling time frames, potentially resulting in higher degrees of biomechanical fixation (because of faster increase in bone mechanical properties, despite the same levels of BIC) at earlier times *in vivo*.^{32–35}

It has been hypothesized that the dissolution of calcium- and phosphorous-based deposits may play a role in the bioactivity of the surfaces, and that bioactivity enhancement leads to early bone tissue formation rate around the implants.⁷ Considering the deposition thickness (20–50 nm), composition, and microstructure (amorphous) used in the present study (see Figure 3B), high dissolution rates were expected to occur for the IBAD-modified implants.^{7–9,20} Therefore, the time-dependent increase in osteoactivity observed in the present study was possibly related to the ongoing interaction between bone and the dissolving/resorbing nanothickness coating at early implantation times.

Because of the time-dependent increase in osteoactivity observed at 4 weeks implantation time, our results indicate that the nanothickness coatings may remain for more than 2 weeks *in vivo* in this particular animal model.

The increase in osteoactivity observed for the 4-week test implants may explain previous biomechanical testing results concerning coatings processed by the IBAD⁸ and sputtering methods.^{17,18} These studies^{17,18} showed that coated implants presented improved initial fixation and healing response compared with grit-blasted/acid-etched implant surfaces at early implantation times. It should be noted that the coating thickness utilized in those studies^{8,17,18} were ~1- μ m thick, or about two orders of magnitude thicker than the depositions utilized in this study,¹⁹ and thickness differences may significantly alter the host response to thin-coated implants.^{7,9,32} Thus, biomechanical testing of the implant surfaces utilized in this study is the subject of ongoing research.

The percent BIC for the test and control implants were not significantly different at the early implantation times evaluated, but an indication that wound healing kinetics was altered was shown by the lower percent bone contact at implant surface for the 2-week test implants. Potential causes for this observation may be

the ongoing thin-film coating dissolution at this early implantation time (bone is still interacting with the thin coating).^{7,8,10,32}

While BIC measurements are indicators of biocompatibility and osteoconductivity, it provides little information concerning wound-healing kinetics around surgical implants, and no direct information regarding the bone–biomaterial mechanical properties. Therefore, the increase in osteoactivity around nanothickness coated implants may be especially interesting in cases where rough surfaces without deposition are utilized as control surfaces. Nanoindentation²⁶ of bone around test implants are currently under investigation and may provide further insight on the bone healing/mechanical property evolution around 20- to 50-nm-thick bioceramic depositions onto alumina-blasted/acid-etched implant substrate.

CONCLUSIONS

The results obtained in this study showed that the 20- to 50-nm-thick bioceramic deposition presented biocompatible and osteoconductive properties. A significantly higher overall and site-specific (to 0.5 mm from the implant surface) bone labeling levels for the 4-week test implants were obtained compared with the control surface implants. Despite the early implantation times evaluated, high degrees of BIC were observed for both the test and control implant surfaces.

ACKNOWLEDGMENTS

The authors gratefully acknowledge the invaluable help of Noel Clarke, Patty Lott, and Preston Beck from the Orthopedic Research Laboratory at the University of Alabama at Birmingham.

REFERENCES

1. Albrektsson T, Branemark PI, Hansson HA, Lindstrom J. Osseointegrated titanium implants. Requirements for ensuring a long-lasting, direct bone-to-implant anchorage in man. *Acta Orthop Scand* 1981; 52:155–170.
2. Branemark PI. Osseointegration and its experimental background. *J Prosthet Dent* 1983; 50:399–410.
3. Branemark PI, Hansson BO, Adell R, et al. Osseointegrated implants in the treatment of the edentulous jaw. Experience from a 10-year period. *Scand J Plast Reconstr Surg Suppl* 1977; 16:1–132.
4. Buser D, Broggini N, Wieland M, et al. Enhanced bone apposition to a chemically modified SLA titanium surface. *J Dent Res* 2004; 83:529–533.

5. Lemons J, Dietch-Misch F. Biomaterials for dental implants. In: Misch CE, ed. *Contemporary implant dentistry*. Saint Louis, MO: Mosby, Inc.; 1999:271–302.
6. Liu Y, de Groot K, Hunziker EB. Osteoinductive implants: the mise-en-scene for drug-bearing biomimetic coatings. *Ann Biomed Eng* 2004; 32:398–406.
7. Yang Y, Kim KH, Ong JL. A review on calcium phosphate coatings produced using a sputtering process – an alternative to plasma spraying. *Biomaterials* 2005; 26:327–337.
8. Park YS, Yi KY, Lee IS, Han CH, Jung YC. The effects of ion beam-assisted deposition of hydroxyapatite on the grit-blasted surface of endosseous implants in rabbit tibiae. *Int J Oral Maxillofac Implants* 2005; 20:31–38.
9. Ong JL, Carnes DL, Bessho K. Evaluation of titanium plasma-sprayed and plasma-sprayed hydroxyapatite implants in vivo. *Biomaterials* 2004; 25:4601–4606.
10. Lacefield WR. Current status of ceramic coatings for dental implants. *Implant Dent* 1998; 7:315–322.
11. Lacefield WR. Hydroxyapatite coatings. *Ann N Y Acad Sci* 1988; 523:72–80.
12. deGroot KKC, Wolke JGC, deBieck-Hogervorst JM. Plasma-sprayed coating of calcium phosphate. In: Yamamuro THL, Wilson J, eds. *Handbook of bioactive ceramics, vol. II, calcium phosphate and hydroxyapatite ceramics*. Boca Raton, FL: CRC Press, 1990:17–25.
13. Albrektsson T, Wennerberg A. Oral implant surfaces: part 1 – review focusing on topographic and chemical properties of different surfaces and in vivo responses to them. *Int J Prosthodont* 2004; 17:536–543.
14. Albrektsson T, Wennerberg A. Oral implant surfaces: part 2 – review focusing on clinical knowledge of different surfaces. *Int J Prosthodont* 2004; 17:544–564.
15. Kay J. Calcium phosphate coatings for dental implants. *Dent Clin North Am* 1992; 36:1–18.
16. Kim H, Camata RP, Vohra YK, Lacefield WR. Control of phase composition in hydroxyapatite/tetracalcium phosphate biphasic thin coatings for biomedical applications. *J Mater Sci Mater Med* 2005; 16:961–966.
17. Vercaigne S, Wolke JG, Naert I, Jansen JA. A histological evaluation of TiO₂-gritblasted and Ca-P magnetron sputter coated implants placed into the trabecular bone of the goat: part 2. *Clin Oral Implants Res* 2000; 11:314–324.
18. Vercaigne S, Wolke JG, Naert I, Jansen JA. A mechanical evaluation of TiO₂-gritblasted and Ca-P magnetron sputter coated implants placed into the trabecular bone of the goat: part 1. *Clin Oral Implants Res* 2000; 11:305–313.
19. Coelho PG, Lemons J. In: IBAD nanothick bioceramic incorporation on metallic implants for bone healing enhancement. From physico/chemical characterization to in-vivo performance evaluation. Anaheim, CA, 2005:316–319.
20. Yang CY, Wang BC, Lee TM, Chang E, Chang GL. Intramedullary implant of plasma-sprayed hydroxyapatite coating: an interface study. *J Biomed Mater Res* 1997; 36:39–48.
21. LeGeros RZ, Lin S, Rohanizadeh R, Mijares D, LeGeros JP. Biphasic calcium phosphate bioceramics: preparation, properties and applications. *J Mater Sci Mater Med* 2003; 14:201–209.
22. Donath K, Breuner G. A method for the study of undecalcified bones and teeth with attached soft tissues. The Sage-Schliff (sawing and grinding) technique. *J Oral Pathol* 1982; 11:318–326.
23. Abrahamsson I, Cardaropoli G. Peri-implant hard and soft tissue integration to dental implants made of titanium and gold. *Clin Oral Implants Res* 2007; 18:269–274.
24. Berglundh T, Abrahamsson I, Albouy JP, Lindhe J. Bone healing at implants with a fluoride-modified surface: an experimental study in dogs. *Clin Oral Implants Res* 2007; 18:147–152.
25. Mendes VC, Moineddin R, Davies JE. The effect of discrete calcium phosphate nanocrystals on bone-bonding to titanium surfaces. *Biomaterials* 2007 Nov; 28(32):4748–4755.
26. Butz F, Aita H, Wang CJ, Ogawa T. Harder and stiffer bone osseointegrated to roughened titanium. *J Dent Res* 2006; 85:560–565.
27. Ong JL, Bessho K, Carnes DL. Bone response to plasma-sprayed hydroxyapatite and radiofrequency-sputtered calcium phosphate implants in vivo. *Int J Oral Maxillofac Implants* 2002; 17:581–586.
28. Ong JL, Prince CW, Lucas LC. Cellular response to well-characterized calcium phosphate coatings and titanium surfaces in vitro. *J Biomed Mater Res* 1995; 29:165–172.
29. Coelho PG, Freire JNO, Coelho AL, et al. Bioceramic coatings: improving the host response to surgical implants. In: Liepsch D, ed. *World Conference of Biomechanics Proceedings: Munich, Germany: Medimont, 2006:253–258*.
30. Davies JE. Bone bonding at natural and biomaterial surfaces. *Biomaterials* 2007; 28:5058–5067.
31. Ong JL, Lucas LC. Post-deposition heat treatments for ion beam sputter deposited calcium phosphate coatings. *Biomaterials* 1994; 15:337–341.
32. Lemons JE. Biomaterials, biomechanics, tissue healing, and immediate-function dental implants. *J Oral Implantol* 2004; 30:318–324.
33. Garetto LP, Chen J, Parr JA, Roberts WE. Remodeling dynamics of bone supporting rigidly fixed titanium implants: a histomorphometric comparison in four species including humans. *Implant Dent* 1995; 4:235–243.
34. Roberts WE. Bone tissue interface. *J Dent Educ* 1988; 52:804–809.
35. Chen J, Chen K, Garetto LP, Roberts WE. Mechanical response to functional and therapeutic loading of a retro-molar endosseous implant used for orthodontic anchorage to mesially translate mandibular molars. *Implant Dent* 1995; 4:246–258.

Copyright of Clinical Implant Dentistry & Related Research is the property of Blackwell Publishing Limited and its content may not be copied or emailed to multiple sites or posted to a listserv without the copyright holder's express written permission. However, users may print, download, or email articles for individual use.